Article:
Moorcroft, S orcid.org/0000-0002-4028-2124, Roach, L orcid.org/0000-0002-9166-6662, Jayne, DG orcid.org/0000-0002-8725-3283 et al. (2 more authors) (2020) Nanoparticle-Loaded Hydrogel for the Light-Activated Release and Photothermal Enhancement of Antimicrobial Peptides. ACS Applied Materials & Interfaces, 12 (22). pp. 24544-24554. ISSN 1944-8244

https://doi.org/10.1021/acsami.9b22587

Nanoparticle loaded hydrogel for the light-activated release and photothermal enhancement of antimicrobial peptides

Samuel C. T. Moorcroft[1], Lucien Roach[1], David G. Jayne[2], Zhan Yuin Ong[1,2], Stephen D. Evans[1]**

[1] School of Physics and Astronomy, University of Leeds, Leeds LS2 9JT, United Kingdom
[2] School of Medicine, University of Leeds, Leeds, LS2 9JT, United Kingdom

Keywords: Antimicrobial dressing, hydrogel, lipid coated nanorods, liposomes, antimicrobial peptides, photothermal, stimuli-responsive delivery

ABSTRACT

Rising concerns over multidrug resistant bacteria have necessitated an expansion to the current antimicrobial arsenal and forced the development of novel delivery strategies that enhance the efficacy of existing treatments. Antimicrobial peptides (AMPs) are a promising antibiotic alternative that physically disrupts the membrane of bacteria resulting in rapid bactericidal activity, however clinical translation of AMPs has been hindered by their susceptibility to protease degradation. Through the co-loading of liposomes encapsulating a model AMP, IRIKIRIK-$CONH_2$ (IK8), and gold nanorods (AuNRs) into a poly(ethylene) glycol (PEG) hydrogel we have demonstrated the ability to protect encapsulated materials from proteolysis and provide the first instance of triggered release of AMPs. Laser irradiation at 860 nm, at 2.1 W cm^{-}

^{2}, for 10 mins led to the photothermal triggered release of IK8, resulting in bactericidal activity against Gram-negative *Pseudonomas aeruginosa* and Gram-positive *Staphylococcus aureus*. Furthermore, by increasing the laser intensity to 2.4 W cm^{-2} we have shown the thermal enhancement of AMP activity. The photothermal triggered release, and enhancement of AMP efficacy, was demonstrated to treat two rounds of fresh *S. aureus*, indicating the therapeutic gel has the potential for multiple rounds of treatment. Taken together, this novel therapeutic hydrogel system demonstrates stimuli-responsive release of AMPs with photothermal enhanced antimicrobial efficacy in order to treat pathogenic bacteria.

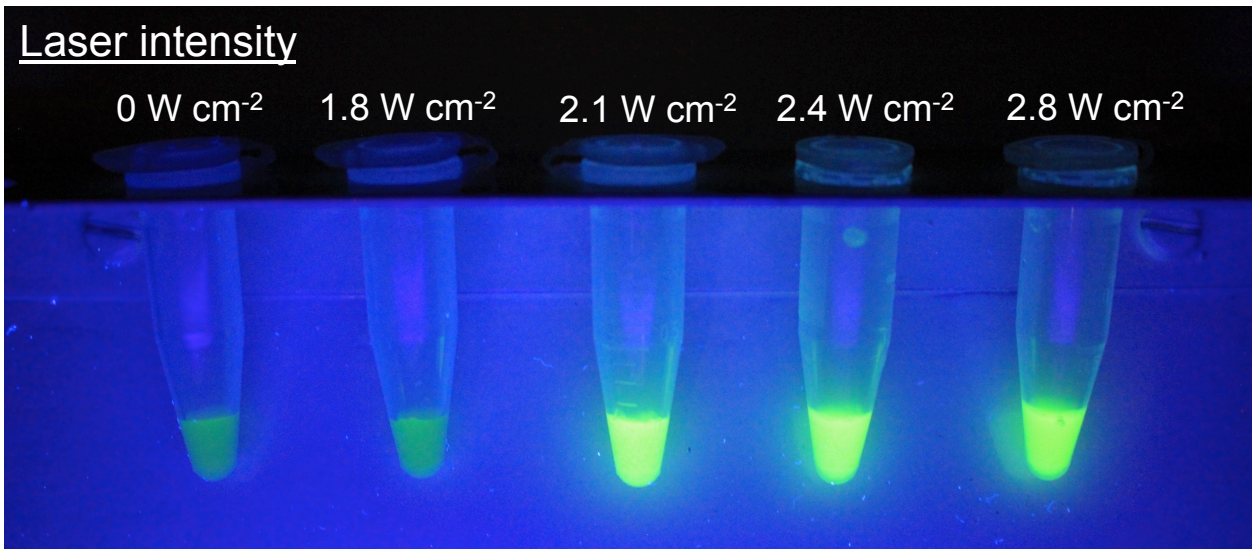

1. Introduction

Societal misuse and overconsumption of antibiotics has led to the emergence of multidrug-resistant bacteria that are set to pose serious global medical, social and economic issues.[1] Such is the threat that bacteria have evolved resistance to "last resort" antibiotics such as carbapenem, leaving critically few options for treatment.[2-3] Naturally derived and synthetic antimicrobial peptides (AMPs) have been identified as a promising antibiotic alternative. AMPs act through the

physical disruption of the bacterial membrane, promoting cytoplasmic leakage, and resulting in rapid bacteria death. Further, the high metabolic cost associated with membrane repair reduces the risk of the emergence of drug resistance.[4-6] However, the clinical translation of AMPs has suffered from the peptide instability and susceptibility to protease degradation *in vivo*.[7-8] As such, the development of protective delivery systems is seen as a key strategy for increasing the chances of AMP implementation.[9-11] However, such systems have primarily focused on the sustained release of AMPs, neglecting stimuli-responsive alternatives.[12-15] Recently, systems utilizing the triggered delivery of antibiotics have drawn widespread attention due to their capacity for spatially and temporally controlled delivery of lethal antibiotic dosages.[16-19] The ability to promote site-specific delivery in response to environmental cues also minimizes systemic loss into peripheral tissues ensuring that local microflora are not subjected to sub-lethal doses that may induce resistance.[4] With the increased treatment efficacy and reduced risk of resistance development, we believe that the implementation of triggered delivery of AMPs could provide the next step toward clinical translation.

In recent years, hydrogels have become increasingly studied as drug delivery vehicles due to the diversity of gel characteristics (e.g. crosslinking density, mesh size, charge, polymer density) that can be controlled to tailor the retention rate of impregnated materials.[20-21] Furthermore, the doping of hydrogels with stimuli-responsive materials has become increasingly popular due to the potential for increasing the accuracy of the location and rate of drug release.[22-24] Traditionally, the fabrication of stimuli-responsive materials has utilized the chemical modification of existing biomaterials, however synthesis of these materials can be complex and difficult to scale-up, leading to increased cost of production and premature leakage of cargo with decreased functionality. [25-26] Such issues can in principle be circumvented by the incorporation

of optically active nanoparticles that, under near-infrared irradiation (NIR), exhibit photothermal heating that can be used to trigger drug release,[27-30] as well as provide thermally induced antimicrobial effects.[31-34] The combination of these treatments has been demonstrated to produce synergistic antimicrobial effects. Meeker *et al.* (2016) developed a daptomycin encapsulating gold nanocage with conjugated staphylococcal targeting proteins, that provided triggered antibiotic and photothermal co-therapy that demonstrated complete bacteria killing of both planktonic suspensions and biofilm models of *S. aureus*.[35] Treatments utilizing the same system without laser irradiation or in the absence of the daptomycin, did not provide complete bacteria eradication.

Liposomes are the most widely researched nanoscale antibiotic delivery system,[36-37] primarily due to their ability to increase the biocompatibility, bioavailability and safety profiles of encapsulated antimicrobial materials.[38] Conventional liposomes predominantly consist of phospholipids, providing an inherent temperature dependent gel-liquid phase transition that increases the membrane permeability. As such liposomal photothermal delivery has been widely demonstrated using dye molecules and anti-cancer chemotherapeutics,[28, 39-41] however equivalent systems to treat infections are lacking. Zhao *et al.* (2018), developed a liposome encapsulating tobramycin that was fabricated using 1,2-distearoyl-*sn*-glycero-3-phosphocholine (DSPC) betainylate cholesterol and the NIR therapeutic cyanine dye, cypate.[42] Irradiation of these liposomes with 808 nm (2 W cm^{-2}) light led to the triggered release of the antibiotic and photothermal bacterial killing that induced a 7- to 8-fold decrease in bacteria viability of a *P. aeruginosa* biofilm compared to free tobramycin. Similar effects may therefore also be achieved utilizing conventional phospholipid liposomes using separate plasmonically active nanoparticles,

thus increasing the variety of liposome compositions available for the photothermal delivery of antimicrobials.

Here, we describe a hydrogel/liposome system for the photothermal triggered release of antimicrobial agents (Figure 1), in which a poly(ethylene glycol) (PEG) based gel containing AMP-loaded liposomes and lipid coated NRs is used for the controlled treatment of bacteria. We have previously shown that the β-sheet forming AMP, IK8, possess potent broad-spectrum antimicrobial activity against various antibiotic-susceptible and antibiotic-resistant microorganisms.[43] However, IK8 was found to be rapidly degraded by proteases such as trypsin and proteinase K, leading to a significant loss in antimicrobial activity.[44] Here we demonstrate that liposomal encapsulation of IK8 protects it from proteolytic degradation. We then added both the IK8 liposomes and the Au nanorods (AuNRs) to the hydrogel and demonstrated the photothermal release of IK8 through laser irradiation at 860 nm (the peak wavelength of the AuNR longitudinal plasmon band). This proved effective for the treatment of both Gram positive and Gram-negative bacteria. Further, by increasing the laser intensity to 2.4 W cm^{-2} (60°C) we found photothermal enhancement of the antimicrobial properties of IK8. Finally, we have shown that the treatment can be repeated in order to highlight the potential for repeated controlled release.

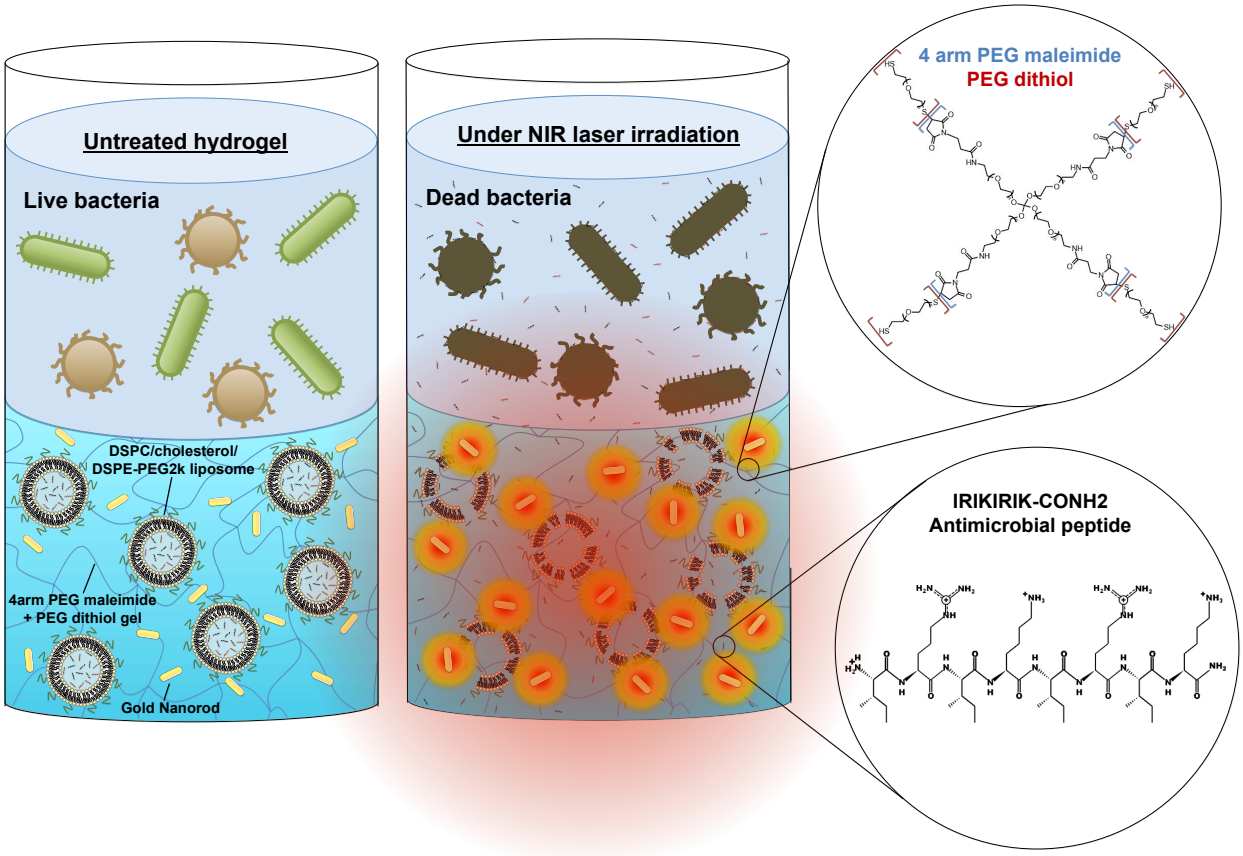

Figure 1. A schematic representation of the PEG-based hydrogel containing gold nanorods and antimicrobial peptide (IK8) loaded liposomes, demonstrating the mechanism for NIR light-triggered release of AMPs.

2. Materials and Methods

2.1 Materials

Phospholipids DSPC and 1,2-distearoyl-*sn*-glycero-3-phosphoethanolamine-N-[methoxy(polyethylene glycol)-2000] (DSPE-mPEG2k) were purchased from Lipoid GmbH

(Ludwigshafen, Germany). Cholesterol, phosphate buffered saline (PBS) and dimethyl sulfoxide (DMSO, analytical grade) was purchased from Merck (Darmstadt, Germany). Mueller Hinton broth II (MHB II), Mueller Hinton agar II, the cell proliferation reagent WST-1, fibroblast growth media and adult human dermal fibroblasts (HDF, Cell Applications Inc. 106-104 05N) were purchased from Merck & Co. (New Jersey, USA). The AMP IRIKIRIK-$CONH_2$ (IK8, > 95% purity) was purchased from GL Biochem Ltd (Shanghai, China). Four-arm poly(ethylene glycol) maleimide (4APM, M_w 20kDa) and poly(ethylene glycol) dithiol (PEGSH, M_w 3.4 kDa) were purchased from Jenkem Technologies USA (Plano, USA). The pathogenic bacteria *S. aureus* (NCTC 12981) and *P. aeruginosa* (NCTC 12903) were obtained from Public Health England Culture Collections.

2.2 Preparation of liposomes and determination of IK8 encapsulation efficiency

Liposomes were prepared according to the thin film hydration method. Briefly, DSPC/cholesterol/DSPE-mPEG2k (65/30/5 mol%) dissolved in chloroform were mixed in a round bottom flask and dried under nitrogen for 1 h. The lipid film was rehydrated in a 1 ml solution of IK8 in PBS (pH = 7.4). The flask was then placed into a water bath preheated to 65°C and gently mixed for 1 h. The resulting multilamellar liposome suspension was then subjected to heated extrusion (65°C) through a 0.4 μm polycarbonate membrane (Whatman, Merck, Darmstadt, Germany) to homogenize the sample. The liposomes were then added to a 15 kDa molecular weight cutoff cellulose dialysis membrane (Biotech) and placed in a 2 liter bath of Milli-Q water which was stirred vigorously for 48 h. The Milli-Q water was replaced after 2, 4, 6 and 24 h. 10 μl of the liposomes were extracted and 10 % v/v of DMSO was added to induce

peptide leakage before the sample was diluted to 300 µl. The solution was then run through an Agilent 1290 series high-performance liquid chromatography (HPLC) system with a 4.6 x 250 mm Insertil ODS-SP column, through which the sample was flowed with an acetonitrile gradient (acetonitrile/water ratio at 0.01 mins 13:87, at 10 mins 100/0) at a rate of 2 µl min^{-1}. A peak was observed at 220 nm after 2.56 mins corresponding to the IK8. The concentration of IK8 encapsulated was determined by integrating the area beneath the peak and comparing this to a predetermined concentration curve (Figure S1).

2.3 Liposome stability testing

2.3.1 Thermal stability

The thermal release of the liposomes was investigated through the release of the self-quenching dye calcein. Liposomes were fabricated through the hydration of lipid films (DSPC/cholesterol/DSPE-mPEG2k, 65/30/5 mol% respectively) using a solution of 0.1 M calcein dissolved in PBS. The resulting liposomes were homogenized using heated-extrusion before unencapsulated dye was removed by passing the liposome suspension through a Sephadex® G-50 gel chromatography column. The first 0.5 ml of sample to pass through the column was collected. The sample was then diluted 2000 times before 200 µl was added to a 96-well plate, for measurement of the sample fluorescence (Exc/Em 496/515 nm). Thermocouples were then added to the wells and the plate was placed in an incubator preheated to 55°C. Once the temperature of the solution had been maintained at 55°C for 5 min the fluorescence was again measured. 1% Triton-X100 was added to the control wells to find the maximum fluorescence, and data normalization.

2.3.2 Liposome leakage

To assess the liposome leakage, 100 µl of calcein loaded liposomes diluted 1000 times was added to a 96-well plate along with 100 µl of MHB II, or MHB II *S. aureus* suspension (initial concentration 1 x 10^6 colony forming units (CFU) ml^{-1}) and incubated at 37°C. The sample fluorescence was measured immediately after preparation and once daily to identify passive leakage of calcein. 1% Triton-X100 was added to the control wells at day 0 and to all wells at the end of the test to identify to determine maximum fluorescence.

2.3.3 Colloidal stability of IK8 Liposomes

Size and polydispersity measurements were performed in triplicate using dynamic light scattering (DLS, Zetasizer Nano ZS) at 25°C. IK8-liposomes diluted 100 times in PBS were sized using a 4mW, 633nm laser with a measurement angle of 173°. In between measurements the liposomes were stored at 4°C.

2.4 Liposomal protection of encapsulated AMP from protease degradation

The efficacy of liposomal encapsulation in protecting the peptide against potential proteolytic degradation was tested by adding 10 µl of the proteolytic enzyme trypsin (50 µg ml^{-1}) to 1 ml of 0.1 mg ml^{-1} free IK8 and IK8-encapsulated liposomes containing the equivalent quantity of peptide. After an hour 150 µl of each sample was removed and the trypsin was inactivated through the addition of 10 µl of 40% w/w trichloroacetic acid.[45] This process was repeated each hour for 5 h. The concentration of IK8 remaining in the samples was quantified using HPLC, liposomally encapsulated IK8 was released by adding 5% v/v DMSO before being added to the HPLC.

2.5 Lipid-coating of AuNRs

Binary surfactant centrimonium bromide (CTAB) and sodium oleate (NaOL) stabilized AuNRs were synthesized as described by Roach *et al*. (2018), these were then lipid coated to increase colloidal stability. The lipid replacement of the CTAB-NaOL bilayer was performed by initially forming a 10 ml suspension of liposomes *via* tip sonicating DSPC/DSPE-PEG2000 (95/5 mol%, 10 mg ml^{-1}) for 2 h before addition to a 10 ml AuNR solution containing 60 μg ml^{-1} of Au. The liposome-NR suspension was then sonicated for 24 h before pelleting using centrifugation (9,000 x g for 30 minutes), removal of the supernatant and re-dispersal in a fresh liposome solution. This process was repeated three times, with the AuNR pellet dispersed into deionized water following the final centrifugation. The dimensions of the AuNRs were determined through transmission electron microscopy (TEM) imaging using a Tecnai G2 Spirit TWIN/BioTWIN with an acceleration voltage of 120 kV. Characterization of the AuNR absorption was measured using a PerkinElmer Lambda 35 spectrophotometer and the Au density was determined using atomic absorption spectroscopy Varian 240 fs (Figure S2d).

2.6 Fabrication of a hydrogel containing IK8-loaded liposomes and AuNRs

Briefly, 4APM was dissolved in 20 μl of 10mM sodium citrate buffer (pH = 6), before addition of lipid coated AuNRs (48 μg ml^{-1} of gold) and liposomes encapsulating 32 μg ml^{-1} of peptide, the suspension was topped up to 40 μl using the citrate buffer. The PEGSH was dissolved into 10 μl of 10 mM citrate buffer and added to a well in a 96-well plate. The 4APM solution, containing the AuNRs and IK8-liposomes, was rapidly added to the PEGSH solution and vortexed to ensure thorough mixing.

2.7 Liposome and AuNR retention within the gel

The retention of liposomes and AuNRs within the hydrogel was determined by incubating the gels with buffer and measuring the leakage of the particles daily. 50 µl PEG gels containing both liposomes and AuNRs were fabricated into opaque 96-well plates and 150 µl of citrate buffer was added to the gels after gelation. To quantify the amount of AuNRs lost from the gel the supernatant absorbance at 860 nm, the longitudinal absorbance wavelength of the AuNRs, was measured. The liposome retention was assessed by including the dye Texas Red within the liposome bilayer, thus providing them with a measurable fluorescence (EX/EM, 561 nm/594 nm). The Texas Red was included by the addition of 0.5 wt% Texas Red to the lipid mixture, prior to the formation of the thin lipid film, the rest of the fabrication protocol was unchanged. The absorbance and fluorescence of the citrate buffer was measured before addition to the gels, and the absorbance and fluorescent values were obtained for the gels on day 0. After 24 hours the supernatant was added to a clean well and the absorbance and fluorescence were both measured, after which the solutions were added back to the gels. The liposome and AuNR release was determined using the equation

$$Release(\%) = 100 \times \frac{X_{Sample} - X_{Buffer}}{X_{Initial} - X_{Buffer}}$$

where X is the fluorescence when of the liposomes or the absorbance of the AuNRs (860 nm).

2.8 Rheometry

The mechanical properties of the IK8-liposome and AuNR loaded gels was assessed using an Anton Paar modular compact rheometer 302. The storage and loss moduli (G' and G'' respectively) of the gels was obtained through applying a constant strain of 1% to the gel and by applying a 1% strain at frequencies of 0.1-100 Hz. A 500 µl gel was fabricated on the bottom

plate of the rheometer that was preheated to 37°C. Immediately after gelation the 25 mm diameter top plate was lowered to 1 mm above the bottom plate before initiating the measurement. Silicon oil was applied to the periphery of the rheometer plates to restrict evaporation from the hydrogel.

2.9 Hydrogel swelling ratios

The swelling ratio is the fractional increase in the weight of the hydrogel due to the absorption of water. PEG gels of 2.5, 5 and 10 wt% were fabricated into the eppendorfs, before freeze-drying. The gels were then weighed before 1 ml of Milli-Q was added. After 10, 30, 60, 120, 180 and 240 mins the excess Milli-Q was removed and the gel was weighed again. The swelling ratio was then calculated using:

$$SR = \frac{W_1 - W_2}{W_2}$$

Where W_1 is the weight of the swollen gel and W_2 is the initial weight of the gel before hydration.

2.10 Cytotoxicity testing

To determine the cytotoxicity of the hydrogel containing IK8-loaded liposomes and AuNRs, 100 µl of fibroblast growth media containing 5×10^3 human dermal fibroblast cells was added to wells of a 96-well plate before incubation at 37°C for 24 h. The fibroblast growth media was replaced with the 90 µl of fresh media and a 10 µl 5 wt% PEG hydrogel containing liposomes encapsulating 32 µg ml^{-1} of IK8 and 48 µg ml^{-1} of AuNRs, fabricated as previously described (Section 2.6), and incubated for a further 24 h The media was then replaced with fresh media

containing 10% v/v of the cell viability reagent WST-1, and incubated for a further 2 h. An equal volume of the media containing 10% v/v WST-1 was added to wells containing no cells to account for the background absorbance by the WST-1 reagent. The media was transferred to wells that did not contain cells and the absorbance was measured at 440 and 660 nm. The relative viability was calculated using the equation given in Figure 2.

$$Relative\ viability = \frac{(OD_{440nm}-OD_{660nm})sample - (OD_{440nm}-OD_{660nm})background}{(OD_{440nm}-OD_{660nm})media - (OD_{440nm}-OD_{660nm})background}\ x\ 100$$

Figure 2. The equation to determine the relative viability of cells treated with a WST-1 assay.

2.11 Triggered release of IK8 and photothermal treatment of pathogenic bacteria

Three distinct gels were fabricated in order to test different properties. One gel contained only AuNRs to test the effects of photothermal heating alone upon the bacterial suspensions. The second gel contained AuNRs and the minimum inhibitory concentration (MIC) of free IK8, to demonstrate the antimicrobial effects of the AMP when delivered alongside the photothermal heating. The third gel contained AuNRs and IK8-loaded liposomes, to demonstrate the triggered delivery of the AMP. All gels were fabricated into wells of a 96-well plate to a total of 50 µl. The wells were topped up to 100 µl with MHB II before the addition of 100 µl of bacteria, $1x10^6$ CFU ml^{-1}. After one h of incubation wells were irradiated with 860 nm laser, at intensities between 1.8 and 2.8 W cm^{-2}, for 10 min. The treated bacteria suspension was subjected to serial dilution before being spread onto agar plates for determination of colony counts relative to the untreated control bacteria incubated in MHB II.

2.12 Repeated treatment of pathogenic bacteria

Hydrogels were fabricated in 96 well plates as described previously, however liposomes containing 2.5 times the MIC of IK8 against *S. aureus* were added to the 4APM solution prior to gelation. The gels were topped up to 100 µl using broth before the addition of 100 µl of *S. aureus* ($1x10^6$ CFU ml^{-1}). The bacteria were left to incubate for 1 h before irradiating at 0, 2.1 or 2.4 W cm^{-2} for 5 mins, before further incubation overnight. The following day the bacteria suspension was removed and colony counting assays were performed to quantify the number of CFUs. The gel was rinsed with 150 µl of PBS before inoculation with 100 µl of fresh *S. aureus* (1.5×10^6 CFU ml^{-1}) before irradiation for 10 min using the same laser intensities in both treatment events. The samples were then incubated for 18 h before being plated onto agar plates for determination of colony counts as described in section 2.8.

2.13 Statistical analysis

All statistical analysis was performed using two-tailed student's t-testing. Results where considered as statistically significant when $P < 0.05$, all significant results are denoted with asterisks with the probability range denoted in the corresponding figure caption.

3. Results and discussion

3.1 Liposomal formulation and IK8 release

To determine the efficacy of the liposomal AMP reservoirs, the different key aspects of thermal, colloidal and enzymatic stability were assessed. Firstly, the passive leakage and thermal stability of liposomes with varying cholesterol content were investigated. Liposomes consisting of DSPC/DSPE-PEG2k containing 0 – 30 mol% cholesterol were loaded with the self-quenching

dye calcein and incubated in MHB II, at 37°C. Increasing the cholesterol concentration was found to significantly reduce the amount of passive leakage over a four-day observation. After the fourth day complete leakage of encapsulated calcein was observed from liposomes without cholesterol (Figure 3a), whereas those containing 10 and 20 mol% cholesterol exhibited leakage of 74 and 58% respectively, and liposomes containing 30 mol% cholesterol displayed negligible leakage. The reduction in permeability is due to the cholesterol molecules introducing conformational ordering of the lipid chains and creating a denser more rigid, barrier for the calcein to cross.[46-48] Little leakage (<5%) was observed when these liposomes were incubated in 5 mM of IK8, in PBS, or in the presence of HDF cells (Figure S3), meaning that neither the AMP nor the presence of mammalian cells interact adversely with the liposome bilayer. As such, we deemed the 30 mol% cholesterol liposomes the most appropriate due to their high retention of encapsulated materials. The thermal stability of the liposomes was assessed by following calcein release when heated above the gel-fluid phase transition temperature (T_m), 55°C for DSPC, for a period of 5 minutes. Increasing the cholesterol content from 20 to 30 mol% resulted in a decrease in calcein release from 55% to 16% (Figure 3b). However, when heating the liposomes containing 30 mol% cholesterol to 55°C in the presence of *S. aureus,* an increased release was observed with 55 ± 6% of the dye released, substantially more than from heating or the bacteria individually, 16 ± 2% and 25 ± 5% respectively. As such, 30 mol% cholesterol liposomes demonstrate high retention of encapsulated materials and an adequate release profile and were therefore taken forward for testing as AMP reservoirs.

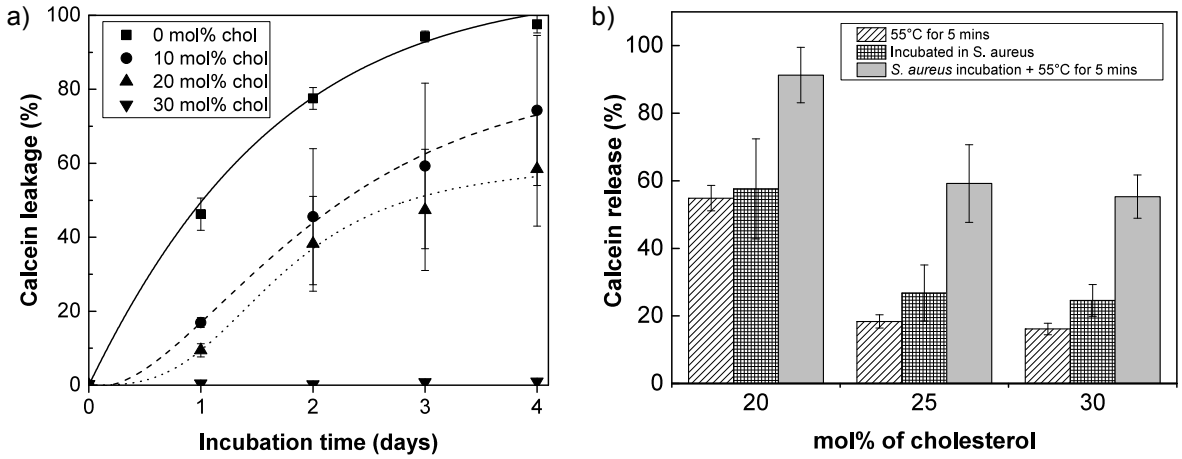

Figure 3. (a) Passive calcein leakage from DSPC/cholesterol/DSPE-PEG2k liposomes with varying cholesterol content when incubated for 4 days at 37°C in MHB II. Error bars indicate the standard deviation (*n*=6). Lines are guides to the eye. (b) Calcein release from liposomes containing 20-30 mol% cholesterol, upon heating to 55°C for 5 mins (diagonal striped), incubation with *S. aureus* (hashed) and heating to 55°C in the presence of the bacteria (solid grey). 100% calcein release was determined through the addition of 1% Triton X-100 to the liposome samples in each environment on day 0. Error bars indicate the standard deviation (*n*=6).

Next the liposomal encapsulation efficiency of IK8 was assessed to ensure sufficient loading of the AMP at bactericidal concentrations. The IK8 concentration in the solution used to hydrate the lipid film was varied and a concentration of 5 mg ml^{-1} enabled the encapsulation of 770 ± 21 µg ml^{-1} of IK8 (Figure 4a), approximately 24 times the minimum inhibitory concentration (MIC) against *S. aureus* (32 µg ml^{-1}, Figure S4), whilst providing low sample-to-sample variability, compared to film-hydration using higher IK8 concentrations. The mass of encapsulated IK8 increased linearly with the concentration of IK8 used to hydrate the lipid film, however, the proportion of the initial IK8 added to the lipid film that is encapsulated decreases causing a drop

in the encapsulation efficiency from 24 ± 4% to 13 ± 2%. The resulting liposomes showed excellent colloidal stability with little change in size upon incubation in PBS at 4°C, over a three-week observation period (Figure 4b). Post fabrication, the liposome diameter was 365 ± 36 nm with a coefficient of variation (CV) of 0.12 ± 0.05, whereas after 3 weeks the liposome diameter increased slightly to 385 ± 42 nm (CV = 0.17 ± 0.04).

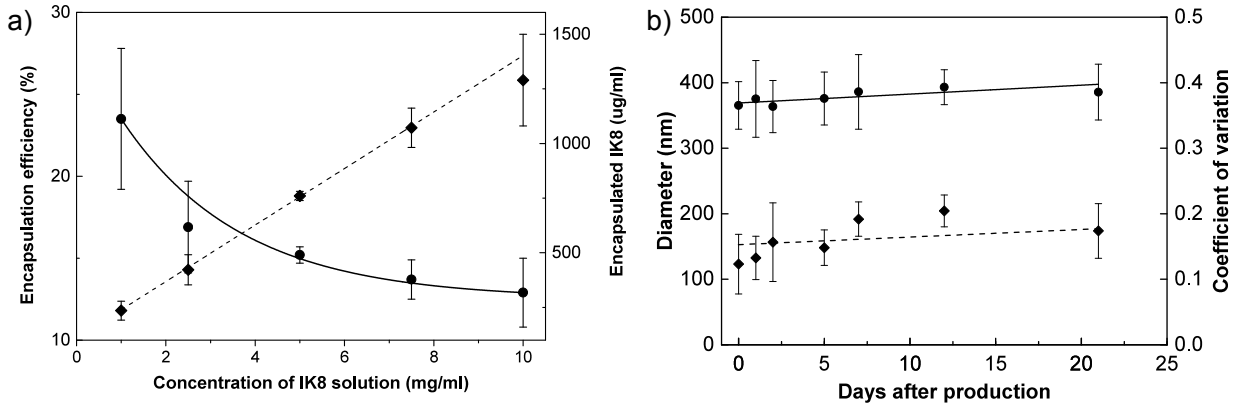

Figure 4. (a) Liposome encapsulation efficiency (circles) and mass of encapsulated peptide (diamonds) upon increasing the concentration of IK8 used to hydrate the thin lipid film during liposome fabrication. Error bars indicate the standard deviation (*n*=3). (b) Diameter of liposomes encapsulating 0.8 mM IK8 (solid line) and coefficient of variation (diamonds) of the liposomes observed over a course of three weeks. Error bars indicate the standard deviation (*n*=3).

The final stage of testing was to assess the efficacy of encapsulation against enzymatic degradation. Despite the great potential of AMPs as antibiotic alternatives, clinical translation has been hindered by proteolytic instability *in vivo*.[49] By loading AMPs within delivery vehicles, it is possible to protect the AMP from protease degradation before reaching the infection site, greatly enhancing treatment efficacy.[50] To test the liposomal protection of encapsulated IK8 against degradation we incubated free and liposomal IK8 in a trypsin solution for 5 h. Our data

shows that 81 ± 6% of liposome encapsulated IK8 remained intact, over double that of the free IK8 in solution, 36 ± 2% (Figure 5). The lipid bilayer encapsulating the IK8 therefore provides a protective barrier that restricts access of proteases, thus potentially allowing treatment infection environments that are often rich in such proteolytic enzymes, such as an open wound.[51]

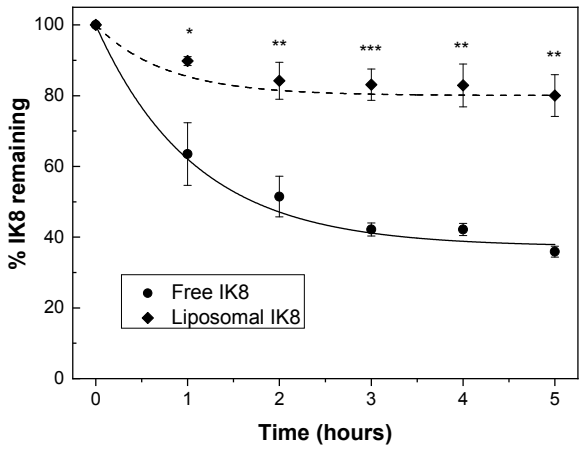

Figure 5. Enzyme degradation of IK8 by trypsin. The IK8 remaining within a sample when 10 µl of 50 µg ml^{-1} of trypsin was added to 1 ml solutions containing 0.1 mg ml^{-1} of IK8 free in solution (solid line) or an equal quantity of IK8 encapsulated within liposomes (dashed line) (*n*=3). p-values indicate; * ≤ 0.05, ** ≤ 0.01, *** ≤ 0.001.

3.2 Hydrogel formation

IK8-liposome / AuNR loaded hydrogels were prepared by mixing the nanoparticles with 4APM as the monomer, before initiating gelation using a PEGSH solution. This gelation occurs through a Michael-type reaction between the maleimide and thiol groups of the two PEG molecules, providing a gel with tunable gelation rates and mechanical properties.[52-54] The PEG hydrogel was also chosen due to its high permeability by small hydrophilic molecules, meaning the gel should

provide minimal interference with the AMP release kinetics.[55] By controlling the pH and the buffer concentration the gelation time could be varied up to two minutes. A 5 wt% gel with a gelation time of 20 seconds was deemed appropriate, as this produced a stiff gel and allowed for a reasonable mixing time. Gels greater than 5 wt% were stiff and difficult to mix, whereas the 2.5 and 1 wt% gels were very ductile almost fluidic, as shown by the small discrepancy between the storage and loss moduli (Figure S5a). The 5 wt% gel also was also advantageous in terms of it's swelling in an aqueous environment. The swelling ratio of the gels was found to decrease as the wt% increased, after 4 hours the 2.5, 5 and 10 wt% gels displayed ratios of 30.4 ± 5.6 (absorbing 41 ± 1 mg of Milli-Q), 22.4 ± 1.8 (59 ± 2 mg of Milli-Q) and 19.0 ± 1.8 (87 ± 6 mg of Milli-Q) respectively, Figure S6. A swelling decrease with the gel wt% has been identified in similar 4 arm PEG hydrogels with comparable swelling ratios.[56] The 5 wt% gel absorption saturated at ~59 mg of liquid, as such the gel, already containing 50 mg of citrate buffer, would only swell to absorb another 9 µl of any liquid added to the gel. The quantity of IK8-liposome solution added to the 4APM solution was determined by quantifying the IK8 concentration and adding the required volume such that upon photothermal stimulation the MIC of IK8 would be released. Alongside the liposomes, 48 µg ml^{-1} of lipid-coated AuNRs (60 x 14 nm, Figures S2a and S2b) were added, as this was the minimum concentration of particles required to heat the sample to 65°C, using a laser intensity of 2.8 W cm^{-2}, at the AuNR longitudinal resonance peak of 860 nm (Figure S2c). Lipid-coated AuNRs were chosen as these showed a significant decrease in toxicity to *S. aureus* compared to the binary surfactant CTAB-NaOL coating used during the synthesis the AuNRs (Figure S5). After treatment with the AuNRs the bacteria were pelleted and the AuNR in suspension were discarded, at the highest concentration we inoculated the bacteria with (250 µg ml^{-1}) the lipid-coated AuNRs did not completely inhibit bacteria

proliferation. The inclusion of peptide-loaded liposomes and lipid-coated AuNRs produced a more malleable gel (Figure S5b) but it did not alter the gelation time and under visual inspection the transparent gel had a slight uniform brown coloration indicating a homogenous distribution of the NRs. The gel also retained the majority of both liposomes and the lipid-coated AuNRs when observed over a 7-day observation with 9 ± 2% and 10 ± 2% released into the surrounding media respectively (Figure S8). The gel transparency also offers the additional benefit of being able to see the wound even after application of the gel, allowing visual identification of an infection.

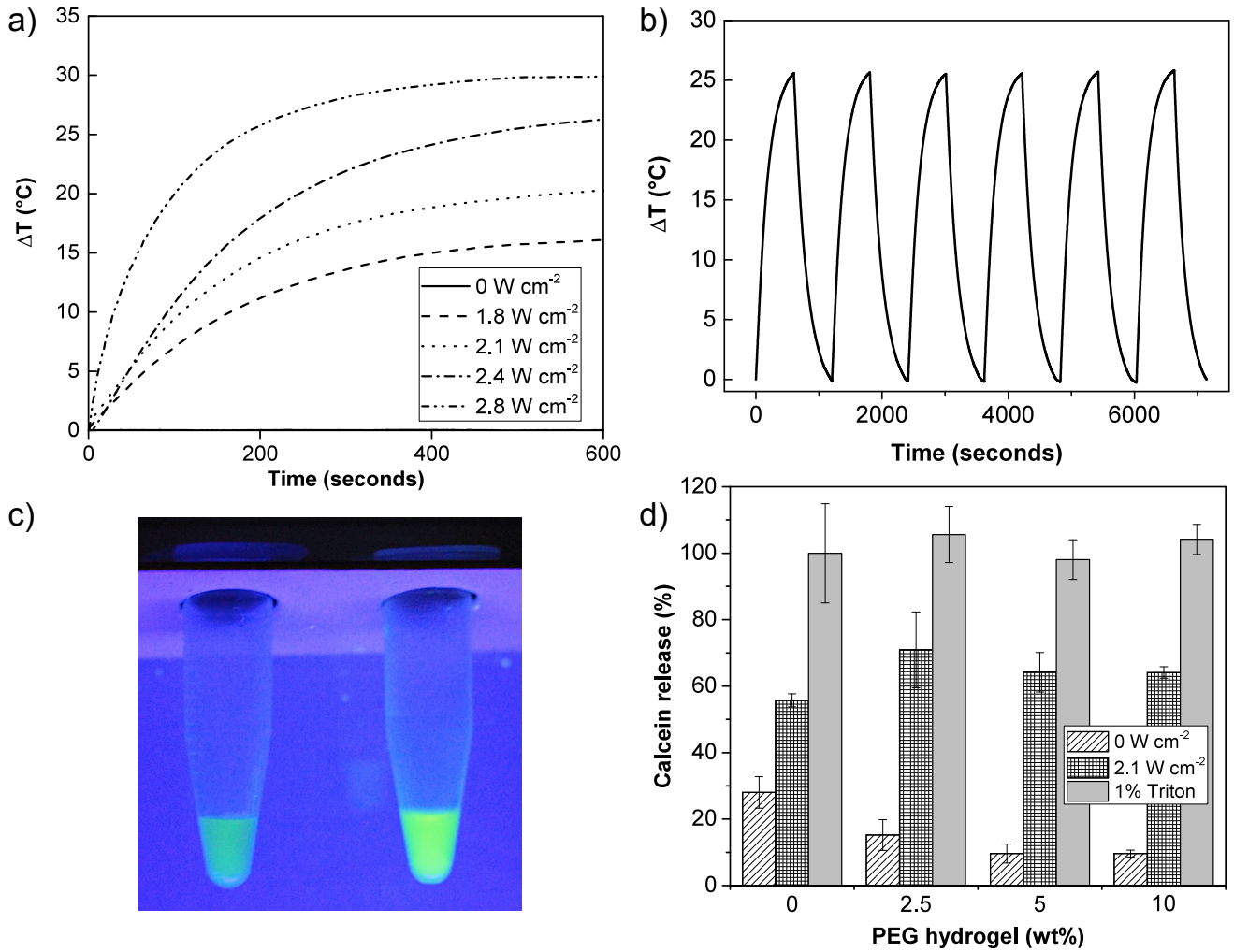

Figure 6. (a) Photothermal heating profiles of the AuNR loaded hydrogel under varying laser intensities for 10 minutes, starting from a base temperature of 35°C. (b) The photothermal heating profile of the NR loaded gel over repeated irradiation cycle at 2.4 W cm^{-2} laser intensity for 10 minutes. (c) AuNR and calcein liposomes loaded into the PEG hydrogel, irradiated for 10 mins at 860 nm with intensities of 0 W cm^{-2} and 2.4 W cm^{-2}, the Eppendorfs on the left and right respectively. (d) Bacterial and photothermal induced release of calcein (diagonal lines and hashed columns respectively) from liposomes in PEG gels of different wt% when incubated in a *S. aureus* suspension. All gels contained 48 μg ml^{-1} of AuNRs and a laser power of 1.4 W cm^{-2} was used to irradiate the samples to 55°C for 5 mins. Error bars indicate the standard deviation (n=6).

The photothermal response of the AuNR-loaded gels was characterized in order to control the thermally induced liposome release of AMPs. The fabricated hydrogels and MHB II were irradiated with a continuous wave laser, 860 nm, at 1.8 – 2.8 W cm^{-2} for 10 min. This gave control of the saturation temperature within the wells to between 50 and 65°C (±1°C) which was reached in 5 mins and maintained for a further 5 min (Figure 6a). The photothermal efficiency was maintained through repeated irradiation cycles (Figure 6b) and the gel containing calcein-loaded liposomes exhibited a visible increase in fluorescence after laser irradiation at 2.4 W cm^{-2} (Figure 6c). These results demonstrate the ability to achieve dose-dependent temperature increases with the NR-loaded hydrogels and provide reproducible levels of heating (with the same temperature attained) over several irradiation cycles. The reproducibility of the heating profiles indicates that there is no change in optical properties and therefore no reshaping or aggregation of the AuNRs under irradiation, at these laser intensities. Subsequently, 64 ± 6% of liposome encapsulated calcein was release when the liposomes were loaded into a 5 wt% gel and

irradiated at 2.4 W cm^{-2}, heating the sample to 55°C, an increase upon the calcein released from liposomes free in suspension, 56 ± 2% (Figure 6d). This increase may be due to the confinement of the liposomes and AuNRs within the 50 µl volume of the gel, rather than when they are free in solution and are able to diffuse throughout the 200 µl total volume of liquid. This would increase the likelihood of the liposomes and thermally radiating AuNRs being in a close proximity to one another making the liposomes more susceptible to thermal destabilization.

3.3 Cytotoxicity of the therapeutic gel

Considering the cytotoxicity of any dressing used on a wound susceptible to infection is of vital importance. Hindering the regenerative process through increasing the toxicity to mammalian cells leaves the wound vulnerable to infection and increases the risks of a wound becoming chronic.[57] As such, the cytocompatibility of the therapeutic gel was assessed using HDF cells; which play a critical role in the formation of granulation tissue.[58] Incubation of the HDF cells with the AuNR and IK8-liposome loaded 5 wt% PEG gel for 24 h showed no detrimental effects on cell viability; with > 97% cell viability observed in the formulation used (Figure 7a). Furthermore, no cytotoxicity was observed upon incubation of the HDF cells with either the lipid coated AuNRs or free IK8 in media at concentrations four times greater than those required to fabricate the therapeutic hydrogel (Figure 7b). As such, each component within the therapeutic gel demonstrates excellent biocompatibility indicating that the gel would be suitable for treatment of infections in a vulnerable wound environment. The lack of cytotoxicity of IK8 at concentrations several times the MIC against *S. aureus* potentially allows for the liposomal loading of high concentrations of peptide to provide multiple treatment events, with no risk of toxicity in the event of leakage.

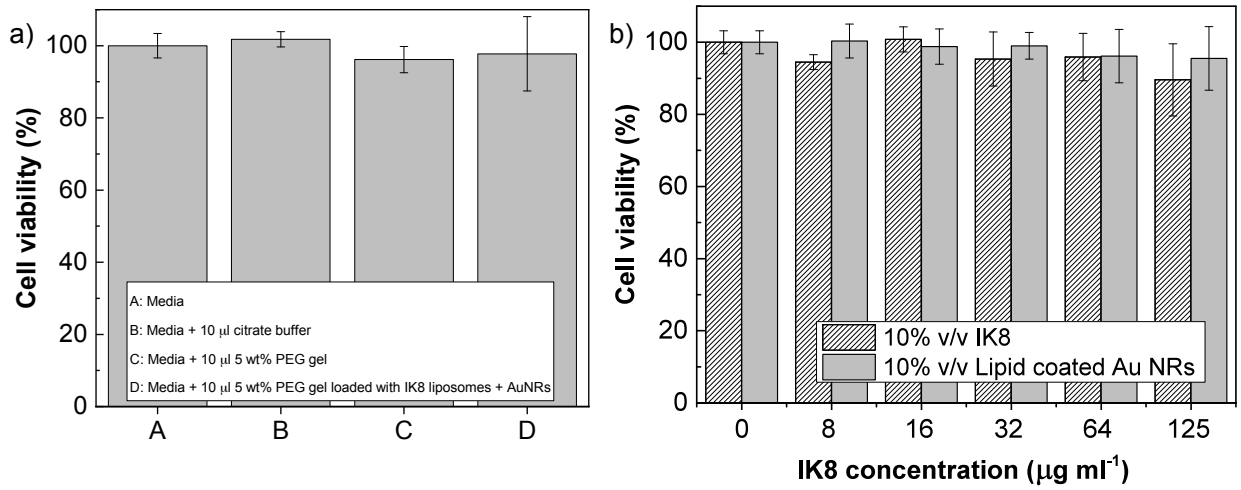

Figure 7. a) Cytotoxicity of the 5 wt% PEG hydrogel and the therapeutic IK8 liposomes-NR loaded 5 wt% PEG hydrogel when incubated with HDFs for 24 h. Error bars indicate the standard deviation (*n*=6). b) The cytotoxicity of lipid coated AuNRs and IK8 in suspension, after 24 h. Error bars indicate the standard deviation (*n*=6).

3.4 Triggered release of IK8 and photothermal treatment of pathogenic bacteria

The antimicrobial properties of the AuNR and IK8-liposome loaded gel were assessed through the treatment of Gram-positive *S. aureus* and Gram-negative *P. aeruginosa*. By controlling the applied laser irradiation intensity between 1.8 and 2.8 W cm^{-2}, we were able to provide photothermal heating profiles between 50 °C and 65 °C and demonstrate the first instance of triggered release of AMPs from liposomes. The triggered release of IK8 was observed to occur for an irradiation of 2.1 W cm^{-2} for 10 minutes and heating the sample to 55°C. This produced 6- and 9-log reductions in the number of CFU ml^{-1} when treating *S. aureus* and *P. aeruginosa* respectively (Figure 8), demonstrating the first instance of triggered release of AMPs to incite bactericidal activity. No decrease in bacteria viability was observed when treating either bacteria

with a laser intensity of 1.8 W cm^{-2}, 50°C. This clearly indicates that the sample must be heated to the lipid gel-fluid phase transition temperature of DSPC (55°C) in order to trigger release of encapsulated materials.[59-61] The thermally induced release is highest close to the phase transition temperature, T_m, due to the coexistence of both gel and fluid domains, producing grain boundaries that have an increased permeability of hydrophilic molecules.[62-63] The liposomal release of the MIC of IK8 showed a similar level of bactericidal activity as the gel containing the MIC of free IK8 against both bacterial types, ~5.5- and ~6.7-log reductions in CFU ml^{-1} against *S. aureus* and *P. aeruginosa* respectively. This indicates that the liposomal encapsulation and subsequent triggered release did not affect the peptide's antimicrobial efficacy. When taken together with the liposomal protease protection, these results indicate that this therapeutic gel offers a potential means of maintaining AMPs in a protease rich wound environment until required, with no decrease in bactericidal efficacy upon triggered release. By utilizing a photothermal trigger, we are also able to enhance the bactericidal activity of the therapeutic gel by heating the bacteria to higher temperatures. Enhanced bacterial kill was observed when treating both bacteria with IK8 and laser irradiation at 2.4 W cm^{-2} (60°C) for 10 min, leading to a 7.8-log reduction in CFU ml^{-1} of *S. aureus* and complete bacteria killing of *P. aeruginosa*. This is similar to previous observations demonstrating thermal enhancement of antibiotics against planktonic *S. aureus*[35] and *P. aeruginosa*[42, 64]. Furthermore, similar studies of the antimicrobial effects of photothermal heating up to ~50-60°C for 10 mins have been performed *in vivo* on cutaneous wounds and demonstrated no thermally induced damage to peripheral tissues or detrimental effects upon reepithelialization.[65-68] Through the fabrication of gels containing AuNRs only, we also evaluated the antimicrobial effects of photothermal heating alone. Neither bacterial species displayed any decrease in bacteria viability until irradiation at 2.4 W cm^{-2}

(heating to 60°C), at which point there was a 2.6-log decrease in *S. aureus* and a 4.4-log decrease in *P. aeruginosa*. Further increase in the laser intensity to 2.8 W cm^{-2} (heating to 65°C) showed complete antimicrobial killing of both bacterial species in all samples containing the NRs. All bactericidal activity was attributed to the photothermal heating, with no bacteria death observed under irradiation at 2.8 W cm^{-2} in the absence of AuNRs. These results show that the IK8 liposome and AuNR loaded hydrogel has the potential for use as a broad-spectrum antimicrobial treatment that, through the regulation of the applied laser intensity, can not only trigger the release of AMPs, but amplify their antimicrobial effects. By harnessing the photothermal enhancement, the chances of providing non-lethal treatment are reduced and as such this treatment should provide a decreased likelihood of bacterial AMP resistance.

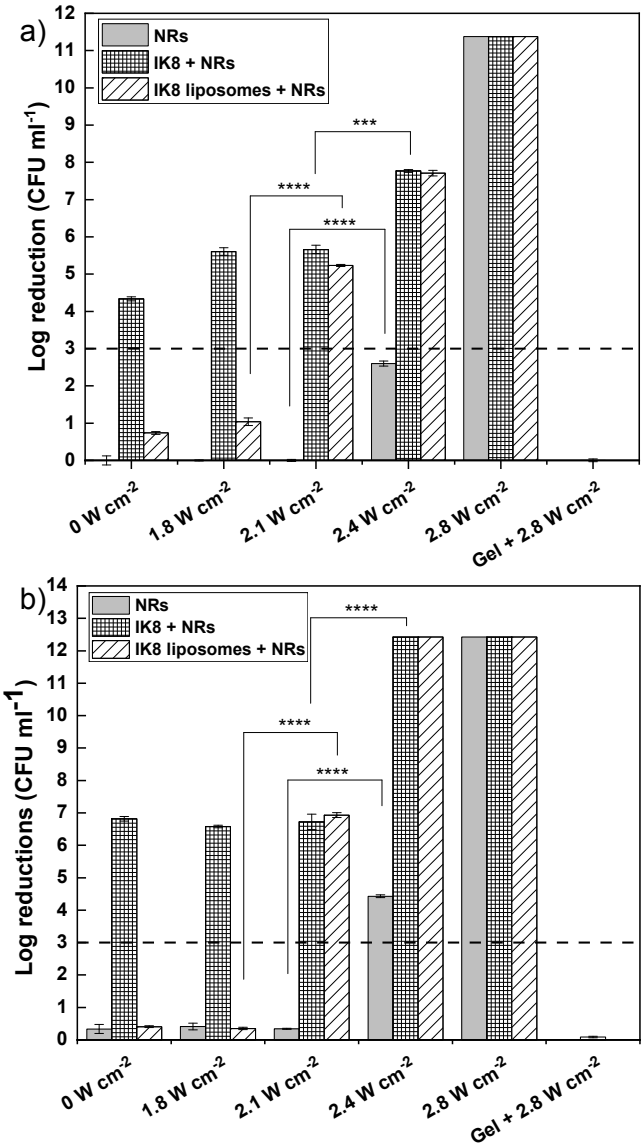

Figure 8. The number of viable (a) *S. aureus* and (b) *P. aeruginosa*, CFU following treatment with gels containing AuNRs, AuNRs and free IK8, and AuNRs with IK8-loaded liposomes, irradiated with an 860 nm laser, at intensities between 1.8 - 2.8 W cm^{-2} for 10 mins. Black dots indicate no CFU remained. Error bars indicate the standard deviation over three independent experiments. p-values indicate; *** ≤ 0.001, **** ≤ 0.0001.

3.5 Repeated treatment of pathogenic bacteria

The ability to utilize the hydrogel as a drug depot to provide repeated triggered release of antimicrobial agents at lethal dosages and in combination with photothermal ablation of bacteria would provide significant advantages in wound management. To demonstrate this, gels were fabricated with AuNRs and an increased number of liposomes such that they contained 2.5 times the MIC of IK8. The gels were inoculated with the first round of *S. aureus* before irradiation at 2.1 or 2.4 W cm^{-2} for 5 mins, resulting in release of 43 ± 8 % of encapsulated materials (Figure S9). The bacteria were then incubated with the gel for 18 h, before removal and quantification of CFU ml^{-1}. The gel was then inoculated with a fresh *S. aureus* suspension and subjected to irradiation at 2.1 or 2.4 W cm^{-2} for 10 minutes, before incubation for 18 h. The second round of bacteria was then removed for CFU quantification. Under irradiation at 2.1 W cm^{-2} (heating to 55°C), the triggered release of IK8 resulted in bactericidal activity over both treatment cycles, with ~7.1- and 3.8-log reductions in *S. aureus* after the first and second cycles respectively (Figure 9). The decrease in antimicrobial efficacy is attributed to the diminishing number of intact IK8-liposomes remaining after each release event. The photothermal enhancement of IK8 can also be observed over both treatments, under irradiation at 2.4 W cm^{-2} (60°C). The photothermal heating produced further 1.1- and 2.5- log reductions in CFUs, in the first and second cycles respectively, compared to systems providing bacteria killing through only AMP delivery. Using a gel containing only AUNRs the difference in photothermal killing was confirmed to be due to the alterations in irradiation time, with the 5 min irradiation in treatment one resulting in a ~0.5-log decrease in CFU ml^{-1} and the 10 min irradiation during treatment two producing a ~2.6-log reduction in CFU ml^{-1}. The bactericidal activity of the gel, both with and without the photothermal enhancement, demonstrates the potential for multiple therapeutic events and can be optimized for a variety of treatments. Furthermore, this indicates that the main

limitation in the number of treatments that can be performed is the concentration of antimicrobial agents encapsulated within the system.

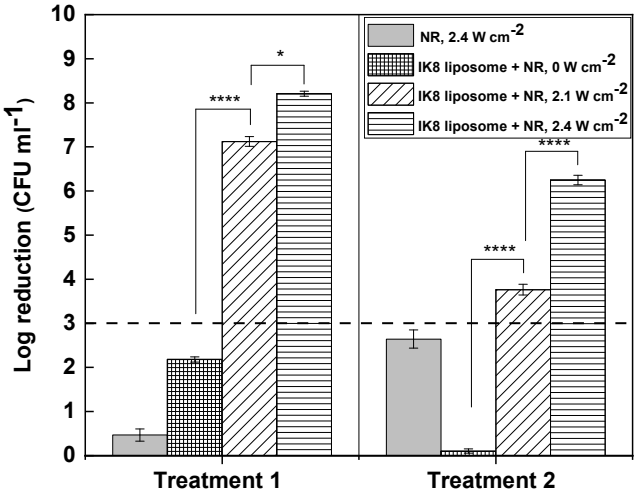

Figure 9. The log reductions in *S. aureus* CFUs over two treatment cycles when treated with the the PEG hydrogel containing 48 μg mL^{-1} of AuNRs irradiated with a laser intensity of 2.4 W cm^{-2} (grey), and gels containing AuNRs and liposomes encapsulating 2.5 times the MIC of IK8 irradiated at 0 W cm^{-2} (hashed), 2.1 W cm^{-2} (diagonal slashed) and 2.4 W cm^{-2} (horizontal lined). Gels were irradiated for a period of 5 mins during the first treatment event and left to incubate for 18 h before being replaced with fresh bacteria and irradiated for 10 mins during the second treatment. Error bars indicate the standard deviation (n=3). p-values indicate; * ≤ 0.05, **** ≤ 0.0001.

4. Conclusion

We have demonstrated a AuNR / AMP liposome loaded hydrogel, that can effectively treat pathogenic bacteria through the photothermal stimulated release of AMPs, which is, to our knowledge, the first instance of triggered release of AMPs in response to exogenous stimuli. Irradiation at 2.1 W cm^{-2} for a period of 10 min caused heating to 55°C, triggering the release of

IK8 resulting in ~6- and ~7-log reductions in the number of Gram-positive *S. aureus* and Gram-negative *P. aeruginosa* CFUs respectively. Increasing the laser intensity to 2.4 W cm^{-2}, heating to 60°C, enhanced the antimicrobial activity of the system with additional 2- and 5-log reductions in viable *S. aureus* and *P. aeruginosa* respectively. Through the optimization of the irradiation time and increasing the number of AMP-loaded liposomes, such that the final concentration of IK8 was 2.5 times the MIC against *S. aureus*, the gel was shown to release bactericidal dosages of AMP to treat two sequential bacterial suspensions, resulting in 7- and 4-log reductions in CFU ml^{-1} from the first and second treatment cycles respectively. Furthermore, irradiation at 2.4 W cm^{-2} demonstrated enhanced antimicrobial activity over both treatment cycles. This demonstrates the capability to perform multiple treatment events using an individual gel, offering a reduced cost per treatment. The liposomal encapsulation of AMPs provides a protective effect against protease degradation, with over 80% of liposome-encapsulated peptide remaining active after a 5-hour incubation with the proteolytic enzyme trypsin. Whilst AMP protection by lipid micelle has previously been documented, this demonstration of the liposomal AMP protection allows the delivery of higher drug doses and opens the door for a wider variety of AMP delivery systems. This gel system would in principle therefore allow the *in vivo* delivery of antimicrobial agents that otherwise are susceptible to degradation. Similar studies have also demonstrated the photothermal destruction of biofilms using nanorod loaded hydrogels,[69] and given the innate antibiofilm properties of IK8[43] we believe that the photothermal enhancement of these properties will be able to continue into the treatment of mature biofilms, which are more representative of infections than treating planktonic bacteria. Taken together, these results indicate that the facile integration of AMP-loaded liposomes and AuNRs into a PEG hydrogel

network offers protection of encapsulated materials and tunable release profiles showing potential for the treatment of infection.

ASSOCIATED CONTENT

Experimental details of MIC testing; HPLC concentration calibration plot of IK8; absorbance spectrum of binary surfactant and lipid coated AuNRs; TEM of lipid coated AuNRs; atomic absorption spectroscopy concentration calibration plot of gold; calcein leakage from liposomes incubated in PBS, 5 mM IK8 and with HDF cells; MIC testing of IK8 on *S. aureus* and *P.aeruginos*; calcein release from liposomes upon varying irradiation time.

AUTHOR INFORMATION

Corresponding Author

* Email: s.d.evans@leeds.ac.uk; z.y.ong@leeds.ac.uk

Present Addresses

†If an author's address is different than the one given in the affiliation line, this information may be included here.

Author Contributions

The manuscript was written with contributions from all authors. All authors have given approval to the final version of the manuscript.

Notes

The authors declare no competing financial interest.

ACKNOWLEDGMENTS

The authors would like to thank the following for financial support: EPSRC (1819417), EPSRC (EP/P023266/1), NIHR (MIC-2016-004), and Royal Society (RSG\R1\180006). S.D.E. acknowledges support from: Engineering and Physical Sciences Research Council (EP/ P023266/1) and the National Institute for Health Research infrastructure at Leeds.

The raw data required to reproduce these findings are available to download from http://review.researchdata.leeds.ac.uk/1295/.

ABBREVIATIONS

AMP: Antimicrobial peptide

IK8: IRIKIRIK-$CONH_2$

AuNR: Gold nanorod

PEG: Poly(ethylene) glycol

NIR: Near infrared

DSPC: 1,2-distearoyl-*sn*-glycero-3-phosphocholine

DSPE-mPEG2k:1,2-distearoyl-*sn*-glycero-3-phosphoethanolamine-N-[methoxy(polyethylene glycol)-2000]

PBS: Phosphate buffered saline

DMSO: Dimethyl sulfoxide

MHB II: Mueller-Hinton broth II

WST-1: Water soluble tetrazolium salt-1

HDF: Human dermal fibroblast

4APM: 4-arm poly(ethylene)glycol-maleimide

PEGSH: Poly(ethylene)glycol dithiol

HPLC: High performance liquid chromatography

CFU: Colony forming unit

DLS: Dynamic light scattering

TEM: Transmission electron microscopy

MIC: Minimum inhibitory concentration

T_m: Phase transition temperature

REFERENCES

1. Medina, E.; Pieper, D. H., Tackling Threats and Future Problems of Multidrug-Resistant Bacteria. In *How to Overcome the Antibiotic Crisis : Facts, Challenges, Technologies and Future Perspectives*, Stadler, M.; Dersch, P., Eds. Springer International Publishing: Cham, 2016; pp 3-33.
2. Geisinger, E.; Isberg, R. R., Interplay Between Antibiotic Resistance and Virulence During Disease Promoted by Multidrug-Resistant Bacteria. *J. Infect. Dis.* **2017,** *215*, S9-S17.
3. Basak, S.; Singh, P.; Rajurkar, M., Multidrug Resistant and Extensively Drug Resistant Bacteria: A Study. *J. Pathog.* **2016,** *2016*, 1-5.
4. Munita, J. M.; Arias, C. A., Mechanisms of Antibiotic Resistance. *Microbiol. Spectr.* **2016,** *4* (2).
5. Lee, J. K.; Luchian, T.; Park, Y. I., New antimicrobial peptide kills drug-resistant pathogens without detectable resistance. *Oncotarget* **2018,** *9* (21), 15616-15634.
6. Zasloff, M., Antimicrobial peptides of multicellular organisms. *Nature* **2002,** *415*, 389-395.
7. Allen, H. K.; Trachsel, J.; Looft, T.; Casey, T. A., Finding alternatives to antibiotics. *Ann. N. Y. Acad. Sci.* **2014,** *1323*, 91-100.
8. Marr, A. K.; Gooderham, W. J.; Hancock, R. E., Antibacterial peptides for therapeutic use: obstacles and realistic outlook. *Curr. Opin. Pharmacol.* **2006,** *6* (5), 468-72.
9. Zetterberg, M. M.; Reijmar, K.; Pranting, M.; Engstrom, A.; Andersson, D. I.; Edwards, K., PEG-stabilized lipid disks as carriers for amphiphilic antimicrobial peptides. *J. Control. Release.* **2011,** *156* (3), 323-8.
10. Brandelli, A., Nanostructures as Promising Tools for Delivery of Antimicrobial Peptides. *Mini-Rev. Med. Chem.* **2012,** *12* (8), 731-741.
11. Nordstrom, R.; Malmsten, M., Delivery systems for antimicrobial peptides. *Adv. Colloid Interfac.* **2017,** *242*, 17-34.
12. Shukla, A.; Fleming, K. E.; Chuang, H. F.; Chau, T. M.; Loose, C. R.; Stephanopoulos, G. N.; Hammond, P. T., Controlling the release of peptide antimicrobial agents from surfaces. *Biomaterials* **2010,** *31* (8), 2348-2357.
13. Parilti, R.; Caprasse, J.; Riva, R.; Alexandre, M.; Vandegaart, H.; Bebrone, C.; Dupont-Gillain, C.; Howdle, S. M.; Jerome, C., Antimicrobial peptide encapsulation and sustained release from polymer network particles prepared in supercritical carbon dioxide. *J. Colloid Interf. Sci.* **2018,** *532*, 112-117.

14. Yang, G.; Huang, T.; Wang, Y.; Wang, H.; Li, Y.; Yu, K.; Dong, L., Sustained Release of Antimicrobial Peptide from Self-Assembling Hydrogel Enhanced Osteogenesis. *J. Biomater. Sci. Polym. Ed.* **2018,** *29* (15), 1812-1824.
15. Kazemzadeh-Narbat, M.; Lai, B. F.; Ding, C.; Kizhakkedathu, J. N.; Hancock, R. E.; Wang, R., Multilayered coating on titanium for controlled release of antimicrobial peptides for the prevention of implant-associated infections. *Biomaterials* **2013,** *34* (24), 5969-77.
16. Moorcroft, S. C. T.; Jayne, D. G.; Evans, S. D.; Ong, Z. Y., Stimuli-Responsive Release of Antimicrobials Using Hybrid Inorganic Nanoparticle-Associated Drug-Delivery Systems. *Macromol. Biosci.* **2018,** *18* (12), 1-14.
17. Kneidl, B.; Peller, M.; Winter, G.; Lindner, L. H.; Hossann, M., Thermosensitive liposomal drug delivery systems: state of the art review. *Int J Nanomedicine* **2014,** *9*, 4387-98.
18. Paliwal, S. R.; Paliwal, R.; Vyas, S. P., A review of mechanistic insight and application of pH-sensitive liposomes in drug delivery. *Drug. Deliv.* **2015,** *22* (3), 231-42.
19. Edson, J. A.; Kwon, Y. J., Design, challenge, and promise of stimuli-responsive nanoantibiotics. *Nano. Converg.* **2016,** *3* (1), 26.
20. Li, J.; Mooney, D. J., Designing hydrogels for controlled drug delivery. *Nat. Rev. Mater.* **2016,** *1* (12), 1-17.
21. Mishra, B.; Upadhyay, M.; Reddy Adena, S. K.; Vasant, B. G.; Muthu, M. S., Hydrogels: An Introduction to a Controlled Drug Delivery Device, Synthesis and Application in Drug Delivery and Tissue Engineering. *Austin. J. Biomed. Eng.* **2017,** *4* (1), 1037.
22. Oliva, N.; Conde, J.; Wang, K.; Artzi, N., Designing Hydrogels for On-Demand Therapy. *Acc. Chem. Res.* **2017,** *50* (4), 669-679.
23. Li, S.; Dong, S.; Xu, W.; Tu, S.; Yan, L.; Zhao, C.; Ding, J.; Chen, X., Antibacterial Hydrogels. *Adv. Sci.* **2018,** *5* (5), 1-17.
24. Gao, W.; Vecchio, D.; Li, J.; Zhu, J.; Zhang, Q.; Fu, V.; Li, J.; Thamphiwatana, S.; Lu, D.; Zhang, L., Hydrogel Containing Nanoparticle-Stabilized Liposomes for Topical Antimicrobial Delivery. *ACS NANO* **2014,** *8* (3), 2900-2907.
25. Mura, S.; Nicolas, J.; Couvreur, P., Stimuli-responsive nanocarriers for drug delivery. *Nat. Mater.* **2013,** *12* (11), 991-1003.
26. Lee, S. M.; Nguyen, S. T., Smart Nanoscale Drug Delivery Platforms from Stimuli-Responsive Polymers and Liposomes. *Macromolecules* **2013,** *46* (23), 9169-9180.
27. Hu, B.; Zhang, L. P.; Chen, X. W.; Wang, J. H., Gold nanorod-covered kanamycin-loaded hollow SiO2 (HSKAu(rod)) nanocapsules for drug delivery and photothermal therapy on bacteria. *Nanoscale* **2013,** *5* (1), 246-252.
28. An, X.; Zhan, F.; Zhu, Y., Smart photothermal-triggered bilayer phase transition in AuNPs-liposomes to release drug. *Langmuir* **2013,** *29* (4), 1061-1068.
29. Mathiyazhakan, M.; Wiraja, C.; Xu, C., A Concise Review of Gold Nanoparticles-Based Photo-Responsive Liposomes for Controlled Drug Delivery. *Nano-Micro Letters* **2017,** *10* (1), 1-10.
30. Gao, G.; Jiang, Y. W.; Jia, H. R.; Wu, F. G., Near-infrared light-controllable on-demand antibiotics release using thermo-sensitive hydrogel-based drug reservoir for combating bacterial infection. *Biomaterials* **2019,** *188*, 83-95.
31. Wang, S. G.; Chen, Y. C.; Chen, Y. C., Antibacterial gold nanoparticle-based photothermal killing of vancomycin-resistant bacteria. *Nanomedicine* **2018,** *13* (12), 1405-1416.
32. Mocan, L.; Matea, C.; Tabaran, F. A.; Mosteanu, O.; Pop, T.; Puia, C.; Agoston-Coldea, L.; Gonciar, D.; Kalman, E.; Zaharie, G.; Iancu, C.; Mocan, T., Selective in vitro photothermal

nano-therapy of MRSA infections mediated by IgG conjugated gold nanoparticles. *Sci. Rep.* **2016,** *6*, 1-9.
33. Yang, N.; Wang, C.; Wang, X.; Li, L., Synthesis of photothermal nanocomposites and their application to antibacterial assays. *Nanotechnology* **2018,** *29* (17), 1-7.
34. Mahmoud, N. N.; Alkilany, A. M.; Khalil, E. A.; Al-Bakri, A. G., Nano-Photothermal ablation effect of Hydrophilic and Hydrophobic Functionalized Gold Nanorods on Staphylococcus aureus and Propionibacterium acnes. *Sci. Rep.* **2018,** *8* (1), 1-10.
35. Meeker, D. G.; Jenkins, S. V.; Miller, E. K.; Beenken, K. E.; Loughran, A. J.; Powless, A.; Muldoon, T. J.; Galanzha, E. I.; Zharov, V. P.; Smeltzer, M. S.; Chen, J., Synergistic Photothermal and Antibiotic Killing of Biofilm-Associated Staphylococcus aureus Using Targeted Antibiotic-Loaded Gold Nanoconstructs. *ACS Infect. Dis.* **2016,** *2* (4), 241-250.
36. Rukavina, Z.; Vanic, Z., Current Trends in Development of Liposomes for Targeting Bacterial Biofilms. *Pharmaceutics* **2016,** *8* (2), 1-26.
37. Basnet, P.; Skalko-Basnet, N., Nanodelivery Systems for Improved Topical Antimicrobial Therapy. *Curr. Pharm. Des.* **2013,** *19* (41), 7237-7243.
38. Vanic, Z.; Holsaeter, A.; Skalko-Basnet, N., (Phospho)lipid-based Nanosystems for Skin Administration. *Curr. Pharm. Des.* **2015,** *21* (29), 4174-4192.
39. Lajunen, T.; Viitala, L.; Kontturi, L. S.; Laaksonen, T.; Liang, H.; Vuorimaa-Laukkanen, E.; Viitala, T.; Le Guevel, X.; Yliperttula, M.; Murtomaki, L.; Urtti, A., Light induced cytosolic drug delivery from liposomes with gold nanoparticles. *J. Control. Release.* **2015,** *203*, 85-98.
40. Agarwal, A.; Mackey, M. A.; El-Sayed, M. A.; Bellamkonda, R. V., Remote triggered release of doxorubicin in tumors by synergistic application of thermosensitive liposomes and gold nanorods. *ACS Nano* **2011,** *5* (6), 4919-4926.
41. Ou, Y. C.; Webb, J. A.; Faley, S.; Shae, D.; Talbert, E. M.; Lin, S.; Cutright, C. C.; Wilson, J. T.; Bellan, L. M.; Bardhan, R., Gold Nanoantenna-Mediated Photothermal Drug Delivery from Thermosensitive Liposomes in Breast Cancer. *ACS Omega* **2016,** *1* (2), 234-243.
42. Zhao, Y.; Dai, X.; Wei, X.; Yu, Y.; Chen, X.; Zhang, X.; Li, C., Near-Infrared Light-Activated Thermosensitive Liposomes as Efficient Agents for Photothermal and Antibiotic Synergistic Therapy of Bacterial Biofilm. *ACS Appl. Mater. Interfaces* **2018,** *10* (17), 14426-14437.
43. Ong, Z. Y.; Gao, S. J.; Yang, Y. Y., Short Syntheticβ-Sheet Forming Peptide Amphiphiles as Broad Spectrum Antimicrobials with Antibiofilm and Endotoxin Neutralizing Capabilities. *Adv. Func. Mater.* **2013,** *23* (29), 3682-3692.
44. Ong, Z. Y.; Cheng, J.; Huang, Y.; Xu, K.; Ji, Z.; Fan, W.; Yang, Y. Y., Effect of stereochemistry, chain length and sequence pattern on antimicrobial properties of short synthetic beta-sheet forming peptide amphiphiles. *Biomaterials* **2014,** *35* (4), 1315-1325.
45. Banerjee, A.; Onyuksel, H., Human pancreatic polypeptide in a phospholipid-based micellar formulation. *Pharm. Res.* **2012,** *29* (6), 1698-1711.
46. Shinoda, W., Permeability across lipid membranes. *Biochim. Biophys. Acta.* **2016,** *1858* (10), 2254-2265.
47. Redondo-Morata, L.; Giannotti, M. I.; Sanz, F., Influence of cholesterol on the phase transition of lipid bilayers: a temperature-controlled force spectroscopy study. *Langmuir* **2012,** *28* (35), 12851-12860.
48. Kraske, W. V.; Mountcastle, D. B., Effects of cholesterol and temperature on the permeability of dimyristoylphosphatidylcholine bilayers near the chain melting phase transition. *Biochim. Biophys. Acta.* **2001,** *1514*, 159-164.

49. Otvos, L., Jr.; Wade, J. D., Current challenges in peptide-based drug discovery. *Front. Chem.* **2014,** *2*, 1-4.
50. Banerjee, A.; Onyuksel, H., Peptide delivery using phospholipid micelles. *Wiley Interdiscip. Rev. Nanomed. Nanobiotechnol.* **2012,** *4* (5), 562-574.
51. Sinclair, R. D.; Ryan, T. J., Proteolytic enzymes in wound healing: the role of enzymatic debridement. *Australas. J. Dermatol.* **1994,** *35* (1), 35-41.
52. Jansen, L. E.; Negron-Pineiro, L. J.; Galarza, S.; Peyton, S. R., Control of thiol-maleimide reaction kinetics in PEG hydrogel networks. *Acta Biomater.* **2018,** *70*, 120-128.
53. Northrop, B. H.; Coffey, R. N., Thiol-ene click chemistry: computational and kinetic analysis of the influence of alkene functionality. *J. Am. Chem. Soc.* **2012,** *134* (33), 13804-13817.
54. Phelps, E. A.; Enemchukwu, N. O.; Fiore, V. F.; Sy, J. C.; Murthy, N.; Sulchek, T. A.; Barker, T. H.; Garcia, A. J., Maleimide cross-linked bioactive PEG hydrogel exhibits improved reaction kinetics and cross-linking for cell encapsulation and in situ delivery. *Adv. Mater.* **2012,** *24* (1), 64-70, 2.
55. Lin, C. C.; Metters, A. T., Hydrogels in controlled release formulations: network design and mathematical modeling. *Adv. Drug Deliv. Rev.* **2006,** *58* (12-13), 1379-1408.
56. Lutolf, M. P.; Hubbell, J. A., Synthesis and Physicochemical Characterization of End-Linked Poly(ethylene glycol)-co-peptide Hydrogels Formed by Michael-Type Addition. *Biomacromolecules* **2003,** *4* (3), 713-722.
57. Wysocki, A. B., Evaluating and Managing Open Skin Wounds: Colonization Versus Infection. *AACN Adv. Crit. Care* **2002,** *13* (3), 382-397.
58. Bainbridge, P., Wound healing and the role of fibroblasts. *J. Wound Care* **2013,** *22* (8), 407-412.
59. Yatvin, M. B.; Weinstein, J. N.; Dennis, W. H.; Blumenthal, R., Design of Liposomes for Enhanced Local Release of Drugs by Hyperthermia. *Science* **1978,** *202* (4374), 1290-1293.
60. Magin, R. L.; Niesman, M. R., Temperature-Dependent Drug Release from Large Unilamellar Liposomes. *Cancer drug delivery* **1984,** *1* (2), 109-117.
61. Li, L.; ten Hagen, T. L.; Schipper, D.; Wijnberg, T. M.; van Rhoon, G. C.; Eggermont, A. M.; Lindner, L. H.; Koning, G. A., Triggered content release from optimized stealth thermosensitive liposomes using mild hyperthermia. *J. Control. Release.* **2010,** *143* (2), 274-279.
62. Papahadjopoulos, D.; Jacobson, K.; Nir, S.; T., I., Phase transitions in phospholipid vesicles-fluorescence polarization and permeability measurements concernint thje effect of temperature and cholesterol. *Biochim. Biophys. Acta* **1973,** *311* (1), 330-348.
63. Cruziero-Hansson, L.; Mourtisen, O. G., Passive ion permeability of lipid membranes modelled via Hpid-domain inteffacial area. *Biochim. Biophys. Acta* **1988,** *944* (1), 63-72.
64. Ricker, E. B.; Nuxoll, E., Synergistic effects of heat and antibiotics on Pseudomonas aeruginosa biofilms. *Biofouling* **2017,** *33* (10), 855-866.
65. Tao, B.; Lin, C.; Deng, Y.; Yuan, Z.; Shen, X.; Chen, M.; He, Y.; Peng, Z.; Hu, Y.; Cai, K., Copper-nanoparticle-embedded hydrogel for killing bacteria and promoting wound healing with photothermal therapy. *J. Mater. Chem. B* **2019,** *7* (15), 2534-2548.
66. Hsiao, C.-W.; Chen, H.-L.; Liao, Z.-X.; Sureshbabu, R.; Hsiao, H.-C.; Lin, S.-J.; Chang, Y.; Sung, H.-W., Effective Photothermal Killing of Pathogenic Bacteria by Using Spatially Tunable Colloidal Gels with Nano-Localized Heating Sources. *Adv. Func. Mat.* **2015,** *25* (5), 721-728.

67. Hu, D.; Li, H.; Wang, B.; Ye, Z.; Lei, W.; Jia, F.; Jin, Q.; Ren, K. F.; Ji, J., Surface-Adaptive Gold Nanoparticles with Effective Adherence and Enhanced Photothermal Ablation of Methicillin-Resistant Staphylococcus aureus Biofilm. *ACS Nano* **2017,** *11* (9), 9330-9339.
68. Yan, L. X.; Chen, L. J.; Zhao, X.; Yan, X. P., pH Switchable Nanoplatform for In Vivo Persistent Luminescence Imaging and Precise Photothermal Therapy of Bacterial Infection. *Adv. Func. Mat.* **2020**, 1909042.
69. Al-Bakri, A. G.; Mahmoud, N. N., Photothermal-Induced Antibacterial Activity of Gold Nanorods Loaded into Polymeric Hydrogel against Pseudomonas aeruginosa Biofilm. *Molecules* **2019,** *24* (14), 1-19.

TABLE OF CONTENTS GRAPHIC